THREE AXIS AMB HIGH SPEED MICRO MOTOR

Alexis Boletis, Hannes Bleuler
Swiss Federal Institute of Technology Lausanne (EPFL)
Laboratory of Robotic Systems (LSRO), 1015 Lausanne, Switzerland
alexis.boletis@epfl.ch

ABSTRACT

This contribution investigates possibilities and limitations of high speed rotation of small rotors supported on active magnetic bearings (AMBs). A sub-millimetric spherical steel ball has reached 2.88 million rpm in partial vacuum. The AMB system actively stabilizes the three translations of spherical rotors with diameters varying from 1 mm down to 0.4 mm. In addition, an interesting method to measure rotational speed is introduced.

INTRODUCTION

High speed rotation of small rotors is needed more and more in many industrial products. Classical products are spindles, turbines for compact devices like scanners, gyroscopes, centrifuge units and so on. The key to achieve high rotating speeds is to have contactless bearings. Active magnetic bearings (AMBs), gas bearings or passive magnetic bearings are possible choices. Gas bearings are not vacuum compatible and passive magnetic bearings have very low damping. We therefore concentrate on AMBs.

The maximum rotating speed achieved ever reported was obtained in 1946 by J. Beams. A 0.795 mm diameter steel rotor of spherical shape reached the speed of $23.16 \cdot 10^6$ rpm in high vacuum conditions (10^{-5} Torr, $1.333 \cdot 10^{-8}$ bar) and exploded under centrifugal stresses. This corresponds to a circumferential speed far higher than what could be expected from available material properties. This effect is probably due to a different stress limit for very small samples as compared to "bulk" materials.

There are some important factors that have to be considered for a high speed motor.

1) During high speed rotation, high centrifugal loads appear inside the rotor. The yield strength of the rotor material fixes the maximum achievable speed without rotor plastic deformation. An optimized geometry and a minimum size of the rotor can reduce the stresses inside the rotor and therefore a higher speed can be reached.

2) As to the induction motor, the iron losses are increased with the operational, hence a high resistive magnetic circuit is needed and magnetic cores should have low hysteresis.

3) Windage losses increase with the square of the speed. Therefore, the system will have to be operated in vacuum.

4) Mechanical losses are the result of vibrations induced by the interactions between the rotor and the stator. An effective suppression of vibrations when the rotor passes critical speeds reduces mechanical losses and therefore higher rotational speeds can be reached.

ROTOR STRESS DURING ROTATION

The centrifugal loads that appear in a rotating solid can lead to failure if the speed is too high. Most common stress-based failure criteria have been based on the assumption of isotropic materials. For 2D stresses and 3D stresses, the Tresca criterion and the von Mises criterion respectively are often used to predict ductile material failure. For the following calculations the von Mises criterion is considered and expressed as (eq. 1),

$$\sigma_{vM} = \frac{1}{2}\left[\left(\sigma_1 - \sigma_2\right)^2 + \left(\sigma_2 - \sigma_3\right)^2 + \left(\sigma_3 - \sigma_1\right)^2\right] \leq \sigma_x \quad (1)$$

where σ_1, σ_2, σ_3 are the principal stresses and σ_x is the yield strength obtained from an uniaxial tensile test.

Expressions for principal stresses in isotropic solid ellipsoids and in solid discs under body forces have already been calculated [2, 3 and 4]. In this paper we will present numerical solutions and comparison between disc shaped rotors and spherical rotors.

It is well known that in a spherical rotor the maximum stress is located in its center (fig. 1). On the contrary, in a cylindrical rotor, the maximum stresses are concentrated at its extremities (fig. 2). In a disc these zones of maximum stresses become one, located in the center as for a spherical rotor (fig. 3). The value of this stress $\sigma_{vM,\max}$ is proportional to the rotor density and to the square of the product between the radius and the rotational speed (eq. 2). The stress $\sigma_{vM,\max}$ must be smaller than σ_x to prevent rotor failure.

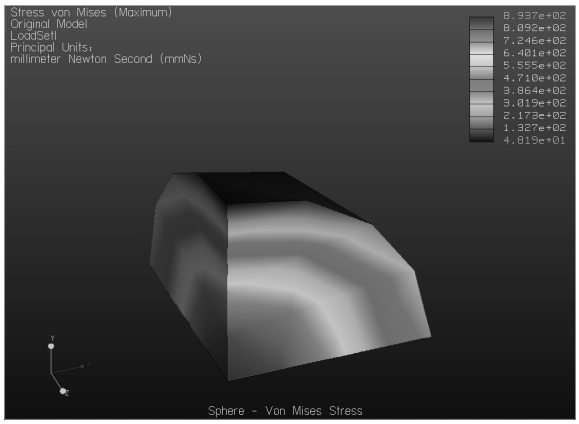

Figure 1 : Stresses in one-eighth of a sphere

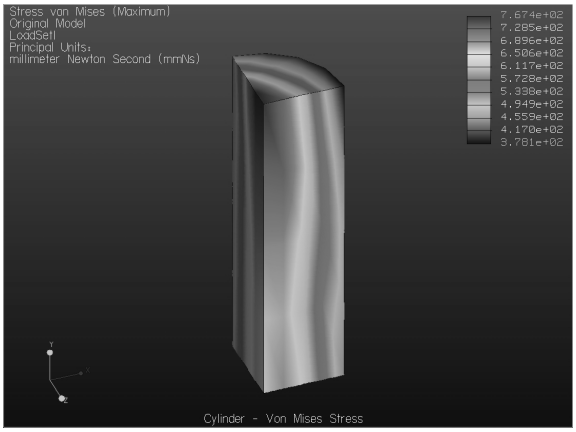

Figure 2 : Stresses in one-eighth of a cylinder

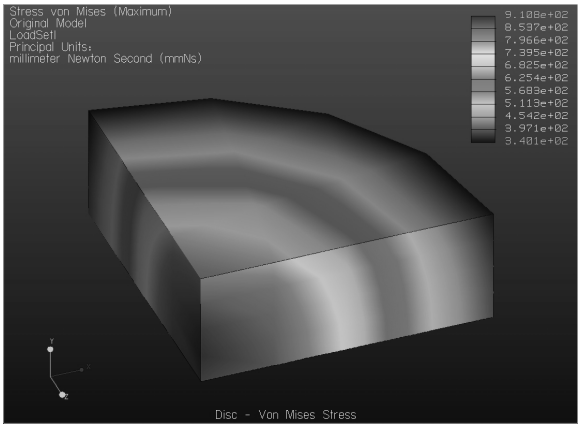

Figure 3 : Stresses in one-eighth of a disc

$$\sigma_{vM,\max} = K\rho\left(r\Omega\right)^2 \tag{2}$$

where:
$\sigma_{vM,\max}$=von Mises stress [N/m^2]
K=shape factor
ρ=density of the material [kg/m^3]
r=radius of the rotor [m]
Ω=rotational speed [rad/s]

To a given yield strength σ_x corresponds a maximum achievable peripheral speed $v_{\max}$ (eq. 3). This speed is constant for a given material and shape and it depends essentially on the yield strength to density ratio.

$$v_{\max} = r\Omega_{\max} = \sqrt{\frac{1}{K}\frac{\sigma_x}{\rho}} \tag{3}$$

Numerical simulations have been carried out to estimate the shape factor K for a spherical rotor, a disc shaped rotor and a cylindrical rotor. Table 1 shows the values of K for different shapes and table 2 indicates the maximum peripheral speed for different materials and shapes.

Shape	***K***
Sphere	0.428
Disc	0.413-0.43
Cylinder	0.43-0.39

Table 1 : Shape factors K

Material	Disc v_{max} [m/s]	Sphere v_{max} [m/s]
Steel (bulk)	330-500	320-480
Carbon fiber comp.	1000-1200	960-1160
Beams steel (thin film)	950-1090	920-1050

Table 2 : Maximum peripheral speed for different materials

It is important to notice that the steel used by J. Beams can not be considered as a "bulk" material but rather as a thin film material (due to the dimension of the sphere). Since the microstructures contain less imperfections than "bulk" structures, the yield strength of "bulk" materials is lower than the yield strength of the same thin film material. Therefore the yield strength and the maximum peripheral speed of rotors made out of thin film steel are higher than rotors made out of "bulk" steel.

MOTOR ASPECTS

Driving a spherical steel rotor with an induction motor is an efficient solution to obtain high speeds (fig. 4). With a minimum of two phases it is possible to drive the rotor clockwise or counterclockwise from a stopped position. If the number of poles pairs is limited to two, the excitation frequency of the two phases corresponds to the frequency of the stator rotating magnetic field and corresponds to the synchronous speed ω_s. The torque can eventually be increased, introducing more pole pairs, but excitation frequency should also be increased to obtain the same frequency of the stator rotating magnetic field.

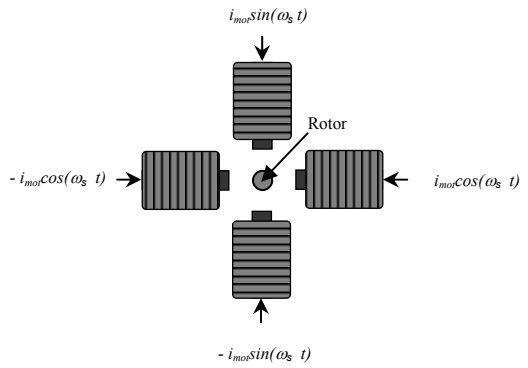

Figure 4 : Two-phase induction motor

At high speeds the motor iron losses and the windage losses become important, limiting rotational speed. Therefore, to limit motor losses, high resistive and low hysteresis coil cores should be used. The only way to limit windage losses is to reduce gas pressure around the rotor, using a vacuum chamber.

The crossing point between the motor torque curve (T_m) and the windage torque curve (T_a), corresponds to the rotational speed ω of the rotor (fig. 5). If the gas pressure is reduced, curve T_a moves to T_{a1} and rotational speed increases from ω to ω_1. Theoretically, if an ideal vacuum is applied, the rotational speed will infinitesimally approach the synchronous speed ω_s. Hence, the maximum achievable rotational speed is limited by ω_s.

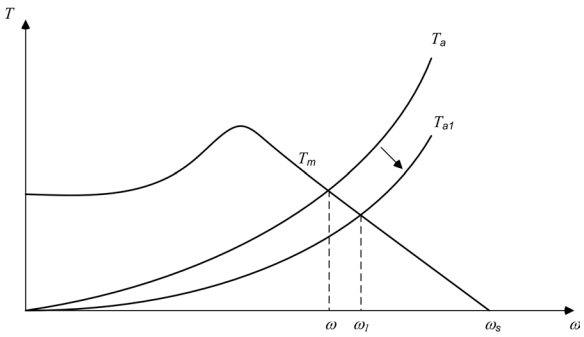

Figure 5 : Crossing point between motor torque and windage torque

For small slips, T_m can be written as follows (eq. 4),

$$T_m = C_m(\omega_s - \omega) \tag{4}$$

where:
C_m is the constant of the motor for a given geometry, excitation frequency and voltage.

Windage torque is proportional to the square of the rotational speed (eq. 5)

$$T_a = C_w \omega^2 \tag{5}$$

where:
C_w is the constant for a given gas, rotor shape and size.

Combining eq. (5) and (6), the expression for the rotational speed ω becomes (eq. 6),

$$\omega = \frac{1}{2}\frac{C_m}{C_w}\left(-1+\sqrt{1+4\frac{C_w}{C_m}\omega_s}\right) \tag{6}$$

The identification of the ratio C_m/C_w can be obtained by applying different excitation frequencies ω_s and measuring rotational speed ω.

THE PROPOSED DEVICE

A magnetic levitation of a spherical rotor is performed with three degrees of freedom control. Five vertically arranged electromagnets (four laterals and one central) create the necessary magnetic forces on a steel sphere with diameter equal or smaller than 1 mm (fig. 6). The external electromagnets are used for radial stabilization and the central electromagnet for axial stabilization. High frequency ferrite cores bring the magnetic field near the suspended sphere and an upper ferrite plate closes it. Ferrite elements are used to limit motor losses due to Eddy currents. As the magnetic fields generated by the external electromagnets are closed through the central electromagnet and the upper plate, the radial forces have not only a horizontal component but also a vertical component.

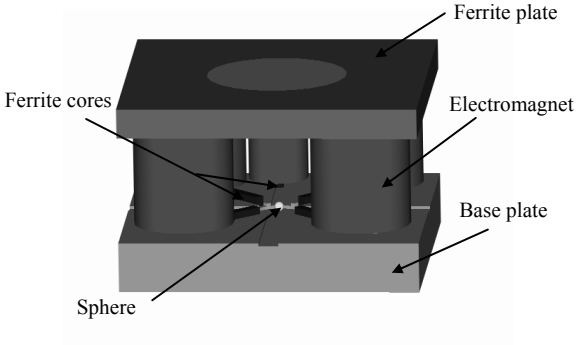

Figure 6 : Setup with the five electromagnets

The position sensing system is composed of two subsystems orthogonally placed in the base plate (fig. 7). Each subsystem contains a red laser source and a 4-segment photodiode that can measure the position of the sphere along two axes (x', z or y', z) [5 and 6]. With the two subsystems it is therefore possible to measure positions x', y', z of the sphere. Afterwards, the x' and y' positions are rotated by 45 degrees to match the principal coordinates system defined by the ferrite cores. The x and y positions are then filtered and fed back to a digital controller as well as the z position.

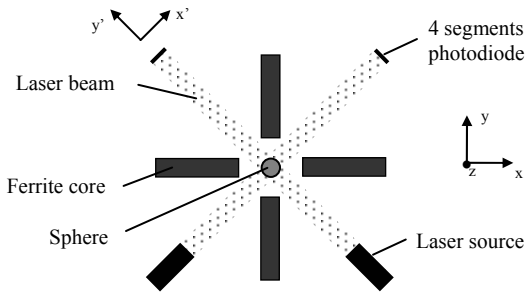

Figure 7 : Position sensing system principle

The response of the sensor along one axis is shown in figure 8. The 4-segments photodiode is considered as a 2-segments photodiode.

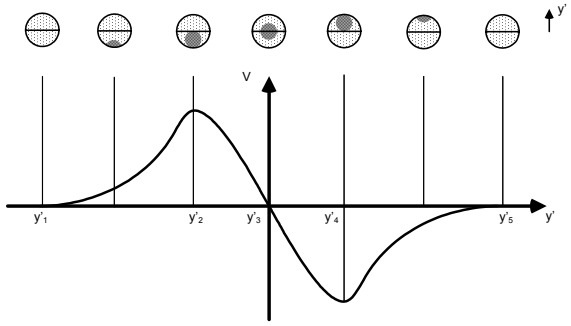

Figure 8 : Position sensor response

The sensor gives a zero output when the sphere doesn't occlude the sensor (y'_1, y'_5) and when its shadow is centered (y'_3). This characteristic presents a good linearity and sensitivity around centered position y'_3, two non linear zones when the sphere shadow is partly outside of the photodiode (y'_1 to y'_2 and y'_4 to y'_5) and two points of zero sensitivity when the sphere shadow is completely inside the upper or the lower segment (y'_2, y'_4). Only the zone around centered position y'_3 is interesting to measure the displacement of the target. In a first approach, the range of this zone corresponds almost to the radius of the sphere.

In order to spin the sphere, a motor function can be added to the radial bearing by superposing a two-phase sinusoidal signal to the bias current i_r and to the control currents i_x and i_y of the electromagnets represented in a horizontal plane (fig. 9).

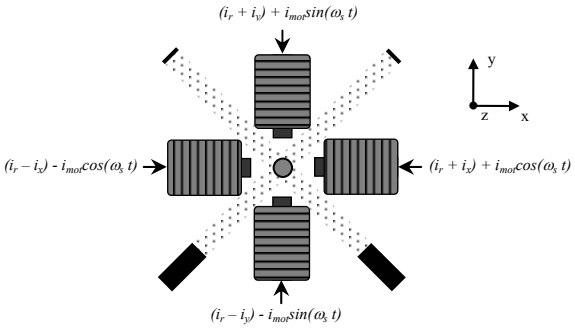

Figure 9 : Motor-bearing combination

SPEED MEASUREMENT

An interesting method is presented here to measure the rotational speed of the rotor. This method do not need any additional sensor since the information about the rotational speed is contained in the position *x*' or *y*' signal given by the position sensing system.

During rotation, the static unbalance of the rotor due to its eccentricity can be detected. This unbalance is synchronous with the rotational speed. For low speeds this unbalance is hardly detectable but since the unbalance increases with the square of the rotational speed [7], at higher speeds the measurement becomes easier. When the rotor is rotating freely around its center of inertia, the unbalance is equal to its eccentricity.

By taking the Fourier transform of the signal *x*' or *y*', different peaks can be identified on the spectrum. The first peak corresponds to the unbalance of the rotor and the next peaks correspond to harmonics due to the rotor shape. During an acceleration of the rotor all these peaks will translate to higher frequencies.

RESULTS

With the realized device, small rotors with diameter down to 0.5 mm have been levitated and spun (fig. 10-11).

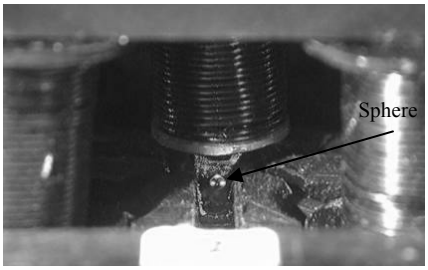

Figure 10 : Levitation of a 0.6 mm diameter sphere

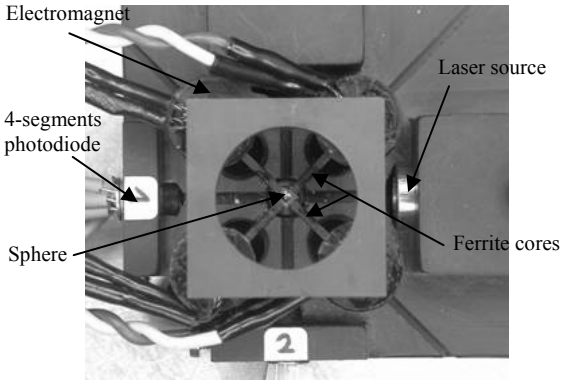

Figure 11 : Top view of the device without the central electromagnet

The maximum reported rotating speed at atmospheric pressure is 186'000 rpm with a 1 mm diameter rotor. The device has also been inserted in a vacuum chamber to increase this speed. At $5 \cdot 10^{-5}$ bar, the 1 mm rotor reached $2.88 \cdot 10^{6}$ rpm.

Speed Measurement

Fourier transform has been applied to the signal *x'* coming out from the position sensing system (fig.12).

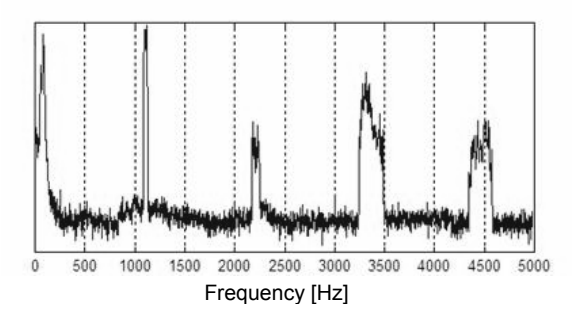

Figure 12 : Fourier transform of position signal *x'*

The highest peak at 1.1 kHz corresponds to the unbalance, next peaks are harmonics. Rotational speed of the rotor during this shot was therefore 66'000 rpm. The peak near to the zero frequency is the 50 Hz noise peak coming from the electrical network.

Identifying the unbalance peak it is more or less difficult depending on the unbalance of the rotor. For a very well balanced rotor, this method will not guarantee good results.

Vacuum measurements

An experiment was made to characterize the rotational speed of two different diameter rotors for different air pressures (fig. 13). Excitation frequency of the two-phase induction motor was 100 kHz and 3V amplitude.

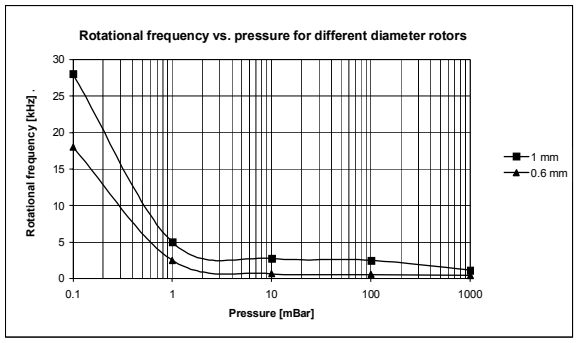

Figure 13 : Tests in vacuum conditions

Pressures smaller than 1 mbar induce an important increase of rotational speed compared to the speed at atmospheric pressure. This is due to the decrease of the coefficient C_w.

It is important to notice that for a 0.6 mm diameter rotor, the speeds obtained in vacuum are smaller than the speeds obtained for a 1 mm rotor. The coefficient C_w of a 0.6 mm rotor is smaller than the C_w of a 1 mm, but the coefficient C_m is even smaller due to the reduced surface of the 0.6 mm rotor and to the increased airgap between stator and rotor.

CONCLUSION AND OUTLOOK

A small device that stabilizes and spins a sub-millimetric spherical rotor (down to 0.4 mm diameter) with a three axis AMB, has been realized. An interesting method based on a Fourier transform to measure rotational speed has been tested.

In vacuum measurement have given a maximum rotational speed of $2.88 \cdot 10^6$ rpm at $5 \cdot 10^{-5}$ bar with a 1 mm diameter sphere.

With our vacuum chamber and our primary pump we were not able to reduce the pressure lower than $1 \cdot 10^{-5}$ bar. To increase the speed of the rotor, a new vacuum chamber has to be designed and a secondary pump has to be added. Some further measurements have to be carried out, in order to identify coefficients C_w and C_m.

REFERENCES

[1] J. Beams, "The Production of High Centrifugal Speeds", J. Appl. Phys., Vol. 17: 886-890, 1946

[2] C. Chree, "The Stresses and Strains in Isotropic Elastic Ellispiod under Bodily Forces derivable from a Potential of the Second Degree", Proc. Roy. Soc. Vol. 58: 39-59, 1895

[3] R. Larsonneur, "Design and Control of Active Magnetic Bearing Systems for High Speed Rotation", Diss ETH No. 9140, Zürich, 1990

[4] G. Schweitzer, H. Bleuler, A, Traxler, Active Magnetic Bearings, Zürich, 1994, ISBN 3 7281 2132 0

[5] A. Boletis, H. Bleuler, "Achieving Ultra-High Rotational Speeds", Proceedings of ISMB8, Mito, Japan, 2002

[6] A. Boletis, L. Sache, S. Menot, H. Bleuler, "Magnetic levitation and rotation of sub-millimetric spherical rotors", Proceedings of MAGLEV2002, Lausanne, Switzerland, 2002

[7] G. Genta, "Vibration of Structures – Practical Aspects", Springer-Verlag, New York, 1993, ISBN 0-387-98506-9